*Progress In Electromagnetics Research C, Vol. 136, 13–22, 2023*

# Compact Reconfigurable Triple Bandstop Filter Using Defected Microstrip Structure (DMS)

**Gomaa M. Elashry[1, 2, *], Abd-El-Hadi A. Ammar[1], and Esmat A. Abdallah[2]**

**Abstract**—In this paper, a low-profile triple-notched bandstop filter (BSF) is introduced. The proposed filter suppresses frequencies of Bluetooth (2.4 GHz), Wi-Max (3.5 GHz), and Wi-Fi (5.2 GHz) using three defected microstrip structures (DMSs). This BSF may be located in the feed line of an ultra-wideband (UWB) antenna. Consequently, not only the complexity is reduced, but also the area of the presented filter ($24 \times 10\,\text{mm}^2$) is plummeted. Multiple rectangular slots are etched in the feed line to achieve multi-notch performance. Additionally, two dumbbell-shaped defected ground structures (DGSs) are etched in the ground plane to improve matching. Three PIN diodes are used to reconfigure the frequency response of the filter. By controlling the three diodes, the proposed filter can support six operating modes. The filter is simulated, optimized, fabricated, and measured to be suitable for cognitive radio applications. It achieves an insertion loss of (40, 29, and 24) dB and a rejection rate of (184, 215, and 277) dB/GHz at 2.4, 3.5, and 5.2 GHz, respectively. The simulated and measured results agree well.

## 1. INTRODUCTION

Nowadays, modern wireless communication systems are causing an increasing demand for multiband and multimode operation antennas. As a result, ultra-wideband (UWB) systems have attracted the attention of researchers [1, 2] due to their high data rate, low cost, and good resistance to multipath and jamming. In UWB and multifunctional communication applications, it is necessary to have bandstop filters (BSFs) [3–5] to suppress any unwanted signal and prevent interference with narrowband technologies such as WLAN.

To design BSFs with two or more attenuation bands, numerous techniques are available, such as coupled lines [6–9], capacitively loaded loops [10], split-ring-coupled microstrip transmission line [11, 12], frequency selective surface (FSS) [13], Archimedean spiral electromagnetic bandgap structure [14], defected microstrip structure (DMS) [15–18], among others. While designing a filter, researchers face some challenges regarding filter characteristics such as obtaining low insertion loss, excellent matching, easy fabrication, and small size. Using the DMS technique guarantees the reduction of the filter size while maintaining good performance because DMS has a high-quality factor, easy design, and easy integration with radio frequency devices. This technique depends on changing the effective inductance and capacitance of the microstrip line by introducing different slots that affect the current distribution [19], thereby changing the frequency response characteristics. In addition, reconfiguration techniques are used to control the characteristics of the frequency response. One of these techniques is radio frequency micro-electro-mechanical system (RF-MEMS), which relies on the mechanical movement of switches to connect or disconnect parts of the antenna [20]. Another technique involves using PIN diodes [21–23], which are more compact and much faster, with switching speeds in the range of 1–100 nsec compared to the RF-MEMS switching speed (in the range of 1–20 μsec) [24].

*Received 18 May 2023, Accepted 28 July 2023, Scheduled 9 August 2023*

* Corresponding author: Gomaa M. Elashry (Gomaa.M.Ashry@eri.sci.eg).

[1] Electronics and Electrical Communications Department, Faculty of Engineering, Al-Azhar University, Cairo, Egypt. [2] Microstrip Department, Electronics Research Institute, Nozha, Cairo, Egypt.

In this study, a triple-notched BSF is proposed using the DMS technique. Triple stopbands are achieved at frequencies of 2.4 GHz (Bluetooth), 3.5 GHz (Wi-Max), and 5.2 GHz (Wi-Fi) using triple DMS structures, which allow for size reduction and low complexity. In addition, to obtain a switchable BSF, the frequency reconfiguration technique is used by integrating three PIN diodes. This paper is organized as follows. Filter geometries, performance, and working principles are presented in Section 2. Section 3 includes the results and discussion. The work is concluded in Section 4.

## 2. PROPOSED FILTER DESIGN

### 2.1. Filter Layout

The aim of this work is to obtain a small size and less complex bandstop filter to suppress signals at frequencies of Bluetooth (2.4 GHz), Wi-Max (3.5 GHz), and Wi-Fi (5.2 GHz). The schematic diagram of the proposed triple stopbands filter is introduced in Fig. 1. The proposed filter is designed on a Rogers RO4003C substrate with $\varepsilon_r = 3.38$, $\tan\delta = 0.0027$, and thickness of 0.81 mm. The three PIN diodes are described as $D_1$, $D_2$, and $D_3$ as shown in Fig. 1(a). The MA4AGP907 PIN diodes (Size: $0.3 \times 0.2\,\text{mm}^2$) are utilized to electrically connect/disconnect the DMS to the BSF. Triple crossed DMSs are etched into the feed line of the antenna to ensures size reduction and generate triple notched rejection bands. Additionally, two dumbbell-shaped DGSs are etched on the ground plane of the proposed filter at input and output ports as illustrated in Fig. 1(b), to enhance the matching of the filter. Table 1 shows the final geometric dimensions of the proposed BSF, which were optimized using the Particle Swarm Optimization technique (PSO) in CST Version 2021.

**Table 1.** Optimized dimensions of the proposed BSF [Unit: mm]

| Symbol | Value | Symbol | Value | Symbol | Value | Symbol | Value |
|---|---|---|---|---|---|---|---|
| $L_s$ | 24 | $W_s$ | 10 | $L_{s2}$ | 11.8 | $W_{s2}$ | 2.4 |
| $L_f$ | 1 | $W_f$ | 1.95 | $L_{s3}$ | 8.5 | $W_{s3}$ | 1.4 |
| $L_n$ | 20 | $W_n$ | 4 | a | 1 | $L_d$ | 1.55 |
| $L_{s1}$ | 17.8 | $W_{s1}$ | 3.4 | $b$ | 1 | $s$ | 0.2 |
| $c$ | 3 | | | | | | |

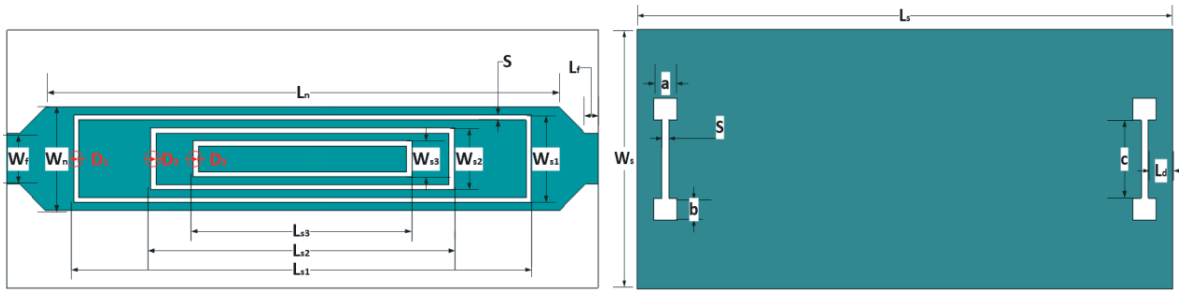


(a) (b)

**Figure 1.** Geometry of the proposed BSF: (a) Front View and (b) Back view.

Figure 2 illustrates the steps by which the proposed BSF is designed along with the $S$-parameters at each step. The main idea is to obtain a BSF in the feed line of the antenna used in cognitive radio applications. Consequently, a transmission line with a wide width ($W_n$) is used to be suitable for etching the DMSs. Firstly, without combining any DMS as shown in Fig. 2(a), there is no notch. Also, increasing $W$ leads to resonant frequency decline. Then, a rectangular ring slot $\text{DMS}_1$ is etched

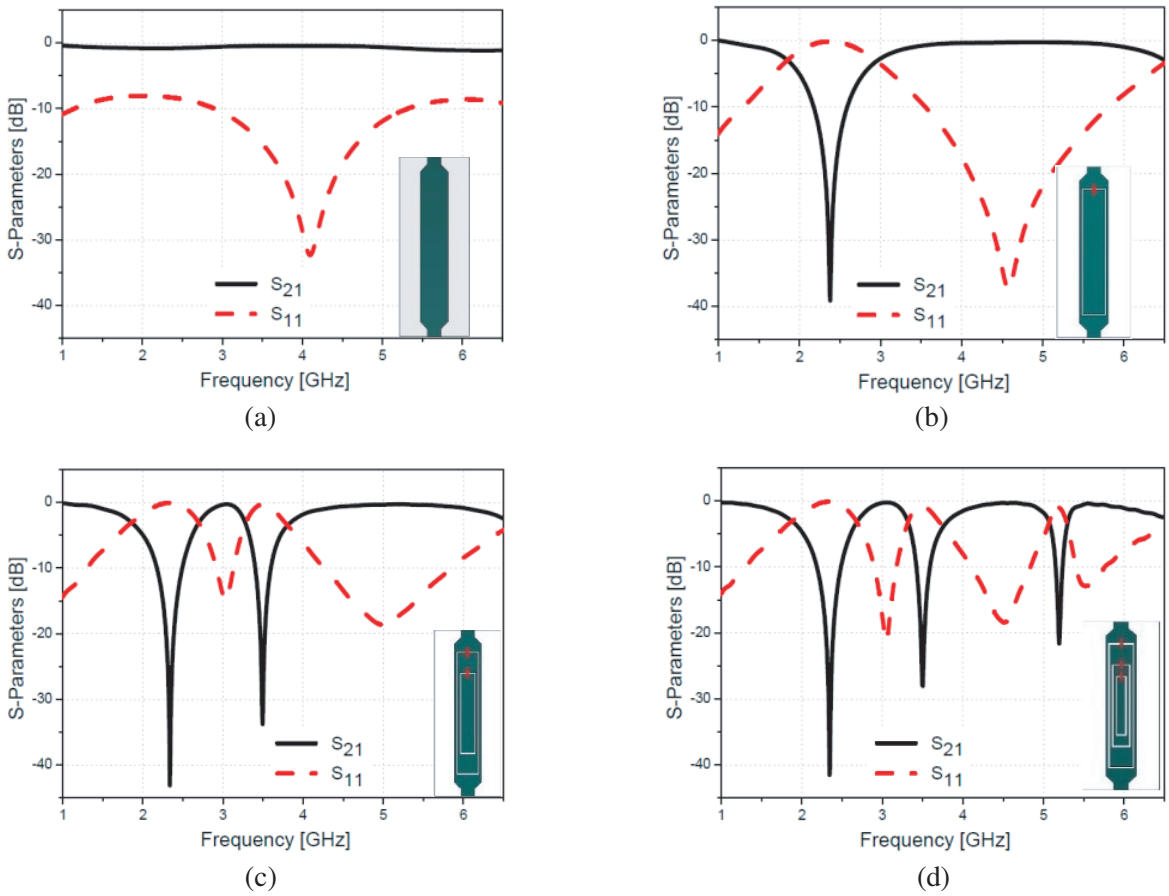


**Figure 2.** $S$-Parameters and the design steps of proposed BSF: (a) feed line without DMS, (b) one DMS at 2.4 GHz, (c) two DMS at 2.4 and 3.5 GHz, and (d) three DMS at 2.4, 3.5 and 5.2 GHz, respectively.

on the line as shown in Fig. 2(b), resulting in a notch at 2.4 GHz. A second rectangular ring slot $DMS_2$ is etched, as shown in Fig. 2(c), leading to a second notch at 3.5 GHz. The third rectangular ring slot $DMS_3$ shown in Fig. 2(d) is also integrated, and a third notch is observed at 5.2 GHz. Each DMS has a length of $(\lambda/2)$ mm, which is calculated from Equation (1) at 2.4, 3.5, and 5.2 GHz, respectively.

$$L_{slot} = \frac{\lambda}{2} = \frac{c}{2f_c\sqrt{\varepsilon_{eff}}} \tag{1}$$

where $c$ is the light velocity in free space, $\varepsilon_{eff}$ the effective relative permittivity, and $f_c$ the stop band center frequency.

Figure 3 illustrates the surface current density distributions for the proposed filter at 2.4, 3, 3.5, and 5.2 GHz, respectively. The filter has the ability to stop the current from reaching port 2 at frequencies of 2.4, 3.5, and 5.2 GHz. The current is stopped at the successive DMS sections. At 3 GHz, for example, the filter has a passband in-between two transmission zeros. One can notice that the current reaches port 2 with the highest intensity. The design parameters' initial values are accurately calculated, followed by their optimization through parametric analysis. Among the various parameters, the most crucial ones that have a substantial impact on the performance are $L_{s1}$, $L_{s2}$, and $L_{s3}$, as depicted in Figs. 4(a), (b), (c).

## 2.2. Equivalent Circuit Model

Using the circuit simulator namely Advanced Design System (ADS), the numerical values are calculated for the equivalent circuit model shown in Fig. 5, with the circuit parameters listed in Table 2. The results

are then compared with the outcomes obtained from (CST) Microwave Studio software. This model consists of many sections as shown in Fig. 5. Feeding line sections at the input and output of the filter, represented by ($L_1$, $C_1$, $L_2$, and $C_2$) logically have $C_1 = C_2$ and $L_1 = L_2$. Two parallel resonant sections ($R_{d1}$, $L_{d1}$, and $C_{d1}$) and ($R_{d2}$, $L_{d2}$, and $C_{d2}$) represent the two dumbbell shapes $R_{d1} = R_{d2}$, $L_{d1} = L_{d2}$, and $C_{d1} = C_{d2}$). Sections ($L_{s1}$, $C_{s1}$, and $C_{s2}$), ($L_{s2}$, $C_{s3}$, and $C_{s4}$) and ($L_{s3}$, $C_{s5}$, and $C_{s6}$) represent the triple DMSs, respectively. Series capacitors ($C_3$, $C_4$, $C_5$, and $C_6$) represent the coupling between DMSs, and ($L_3$, $L_4$, $L_5$, and $L_6$) are shunt inductors corresponding to the thin lines between loops.

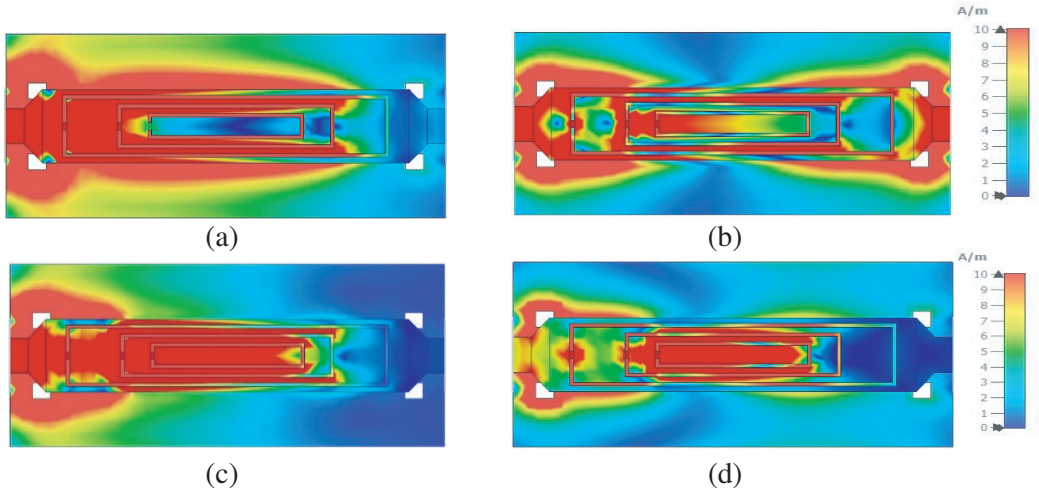


**Figure 3.** Current distributions at (a) 2.4 GHz, (b) 3 GHz, (c) 3.5 GHz, and (d) 5.2 GHz.

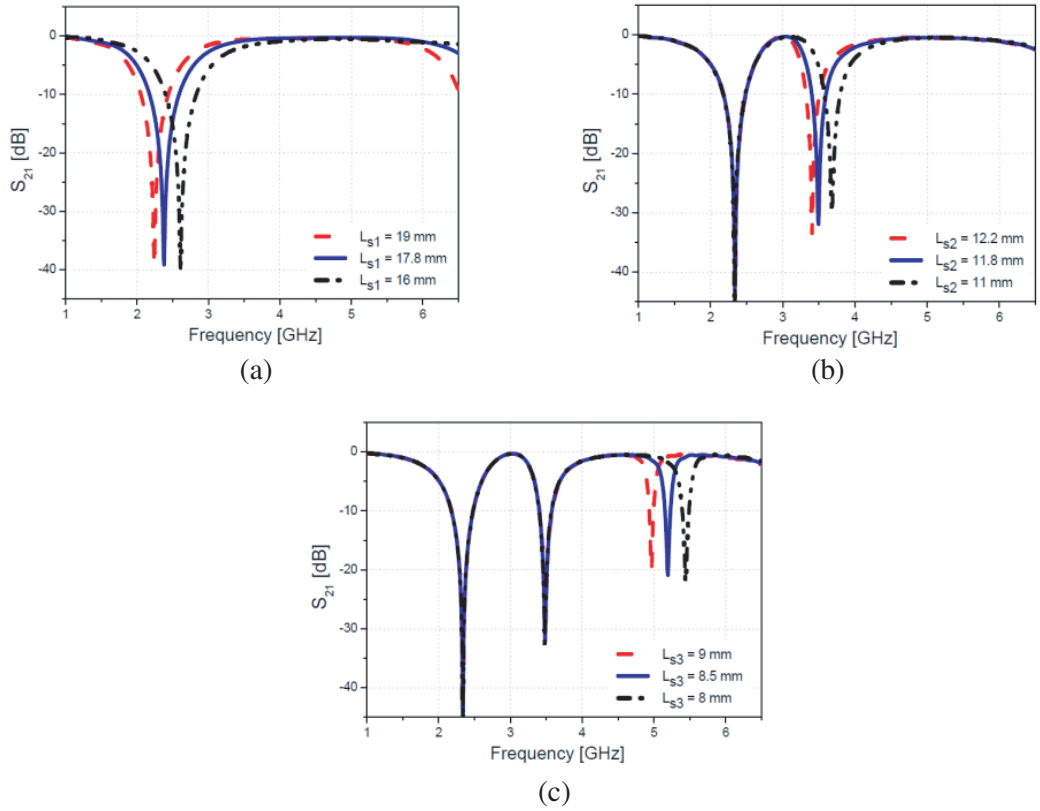


**Figure 4.** The effect of varying, (a) $L_{s1}$, (b) $L_{s2}$ and (c) $L_{s3}$ on the $S_{21}$.

**Table 2.** Passive component values in the equivalent circuit model.

| Component | Value | Component | Value | Component | Value |
|---|---|---|---|---|---|
| $L_1$ | 2.1 nH | $L_6$ | 27.7 nH | $C_{s1}$ | 3.2 pF |
| $C_1$ | 1.1 pF | $C_6$ | 117.087 pF | $C_{s2}$ | 1.818 pF |
| $R_{d1}$ | 0.625 Ω | $L_{s1}$ | 4 nH | $C_{s3}$ | 1.92 pF |
| $L_{d1}$ | 1.2 nH | $L_{s2}$ | 2.4 nH | $C_{s4}$ | 1.6335 pF |
| $C_{d1}$ | 1.35 pF | $L_{s3}$ | 1.728 nH | $C_{s5}$ | 0.864 pF |
| $L_3$ | 10 nH | $C_3$ | 207.077 pF | $C_{s6}$ | 1.49688 pF |
| $L_4$ | 26 nH | $C_4$ | 135.085 pF | $L_5$ | 26.9 nH |
| $C_5$ | 188.779 pF | | | | |

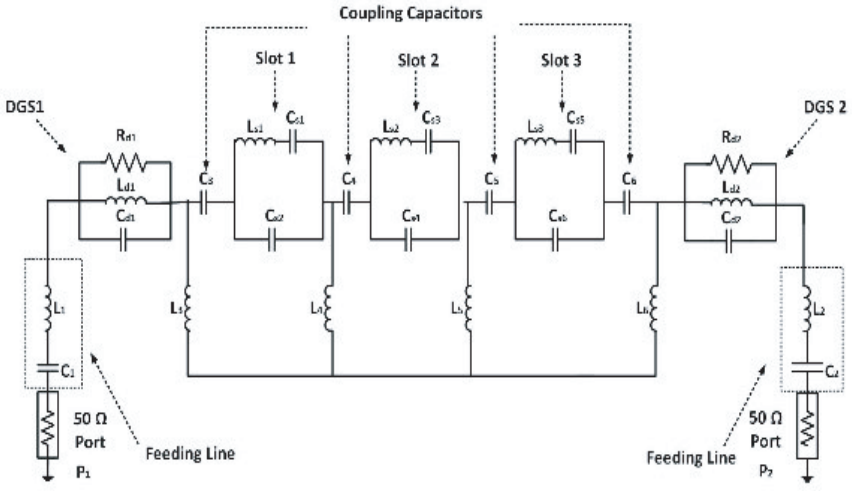


**Figure 5.** Equivalent circuit of the proposed filter layout.

## 3. RESULTS AND DISCUSSION

### 3.1. Comparison Results

The triple stopbands filter has been fabricated as shown in Fig. 6, using the photolithographic technique and measured by ROHDE and SCHWARZ (ZVA67) vector network analyzer. The measurements were conducted using a substrate test fixture, as shown in Fig. 7(a), which reduced filter size by 4 mm. Also, SMA connectors were soldered to reiterate the measurements as shown in Fig. 7(b), and of course good agreement between results was obtained.

Figure 8 shows the transmission coefficient ($S_{21}$) and reflection coefficient ($S_{11}$) of the presented filter. The filter exhibits triple-band rejection characteristics at frequencies of (2.4, 3.5, and 5.2 GHz). From Figs. 8(a) and (b), it is clear that good agreement between simulated and measured results is found. Additionally, insertion loss of (40, 29, and 24) dB and a rejection rate of (184, 215, and 277) dB/GHz are achieved at 2.4, 3.5, and 5.2 GHz respectively.

According to [25], RF circuits with negative group delay (NGD) are beneficial in several analog-signal-processing applications. The group delay response of the filter is shown in Fig. 8(c). The proposed filter exhibits flat passbands of 0.5 ns approximately and an (NGD) of 3, 2.5, and 1.9 ns at 2.4, 3.5 and 5.2 GHz, respectively.

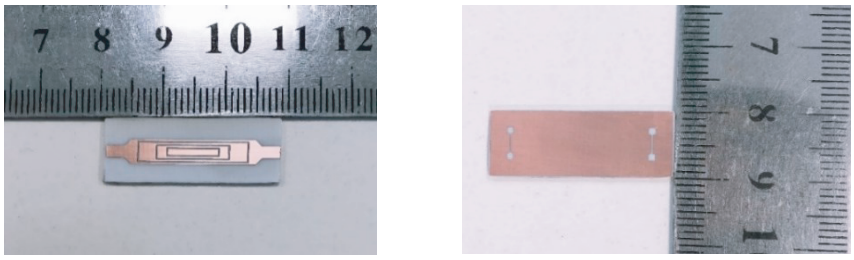


(a) (b)

**Figure 6.** Photograph of the proposed DMS-BSF: (a) Front view and (b) Back view.

(a) (b)

**Figure 7.** Measurements: (a) With substrate test fixture and (b) With connectors.

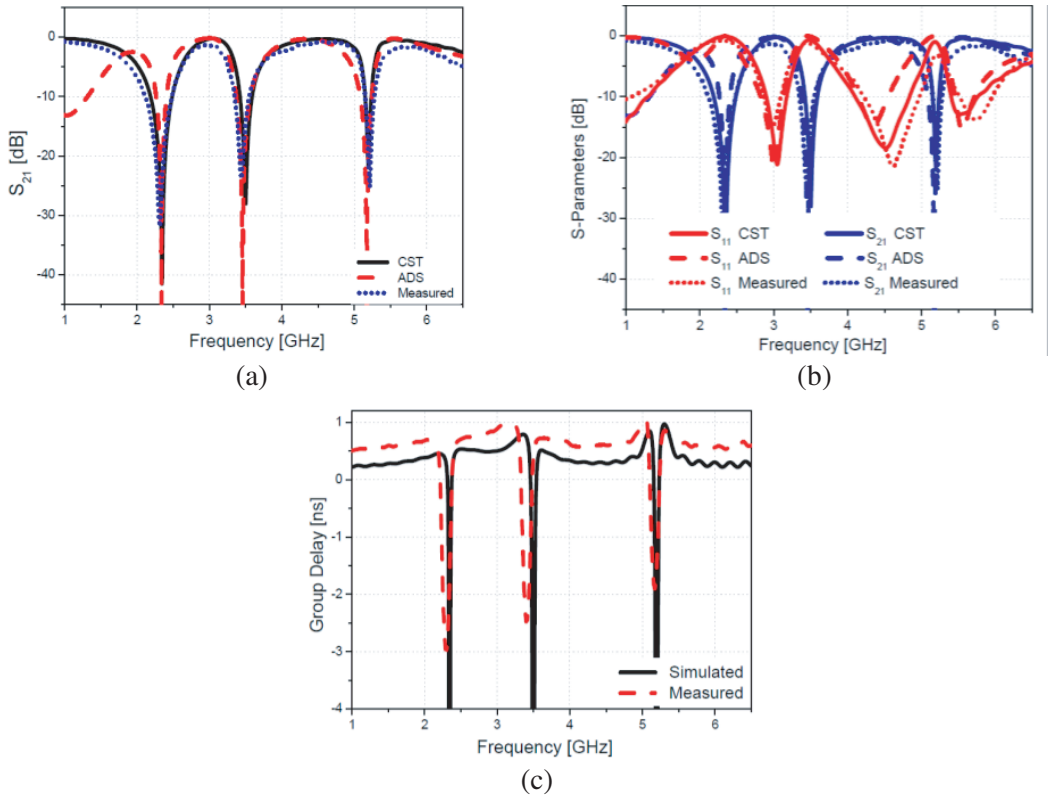


(a) (b) (c)

**Figure 8.** (a) $S_{21}$, (b) $S$-parameter, (c) Group delay of the proposed filter.

### 3.2. Reconfigurability Concept of the Proposed BSF

The characteristics of the three diodes are illustrated in Fig. 9. These diodes work according to the states shown in Table 3. It is obvious that the proposed BSF has three rejection bands (2.4, 3.5, and 5.2 GHz) with all diodes ($D_1$, $D_2$, and $D_3$) ON. The proposed filter has two stopbands in two cases: the first case at (2.4 and 3.5 GHz) when $D_1$ and $D_2$ are ON, but $D_3$ is OFF, and the other case at (2.4 and 5.2 GHz) if $D_1$ and $D_3$ are ON, and $D_2$ is OFF. If $D_1$ is ON, and both $D_2$ and $D_3$ are OFF, only one stopband is available (2.4 GHz) or (3.5 GHz) if $D_1$ and $D_3$ are OFF, but $D_2$ is ON. When all diodes are OFF, the filter acts as a direct transmission line without any notch.

**Table 3.** States of $D_1$, $D_2$, and $D_3$.

| State | $D_1$ | $D_2$ | $D_3$ | Notchat frequency (GHz) |
|---|---|---|---|---|
| **0** | OFF | OFF | OFF | All band pass |
| **1** | ON | ON | ON | 2.4/3.5/5.2 |
| **2** | ON | ON | OFF | 2.4/3.5 |
| **3** | ON | OFF | ON | 2.4/5.2 |
| **4** | ON | OFF | OFF | 2.4 |
| **5** | OFF | ON | OFF | 3.5 |

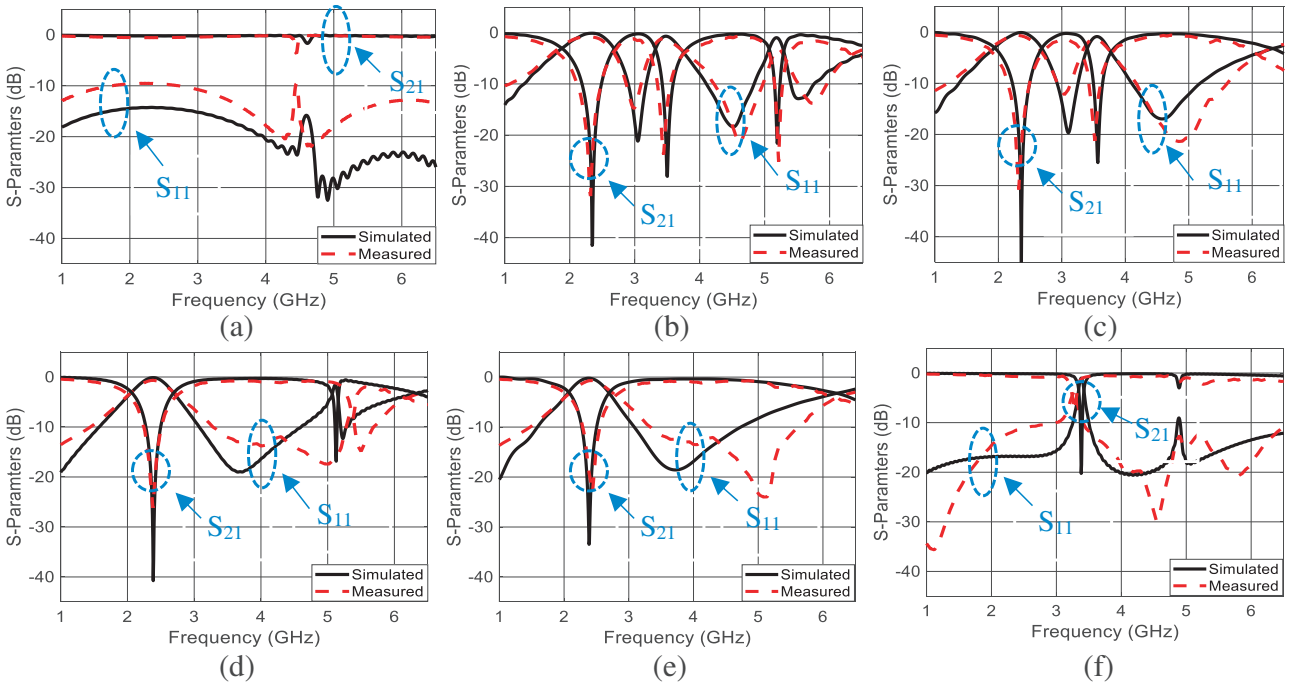


**Figure 9.** $S$-parameters according to $D_1$, $D_2$, and $D_3$ states: (a) state 0, (b) state 1, (c) state 2, (d) state 3, (e) state 4, (f) state 5.

Table 4 lists a detailed comparison of the proposed filter with recently reported BSFs. Based on this comparison, this work proposed a DMS BSF that offers several advantages over other designs. It provides three rejection bands (2.4 GHz, 3.5 GHz, and 5.2 GHz) with sharper rejection levels. Moreover, it has a smaller size (240 $mm^2$) than many other published designs. Additionally, it demonstrates

**Table 4.** Comparison with other reported BSFs.

| Ref. | Design Technique | Rejection Bands (GHz) | Bandwidth (GHz) | Rejection Level (dB) | Size ($mm^2$) | Reconfigurable |
|---|---|---|---|---|---|---|
| [6] | Coupled-Line Stub-Loaded shorted (SIR) | 1.56/2.4/ 3.46 | 0.3/0.7/0.55 | 20/25/38 | 300 | no |
| [10] | Capacitively Loaded Loops (CCLs) | 2.95/3.68 | 0.0745/0.0782 | 15.04/15.1 | 900 | yes |
| [11] | A split-ring-Resonator (SRR) | 4.05/4.75 | NA | 18/15 | NA | yes |
| [14] | Archimedean Spiral Electromagnetic Bandgap Structure | 3.5/5.2/7.4 | 1.07/0.41/0.61 | 35.6/28.2/24.9 | 480 | no |
| [16] | DMS | 3.8/6.7/9.5 | 0.73/0.45/0.31 | 55/36/35 | 741 | no |
| [19] | DMS and Dual-Mode Resonator | 1.56/2.4/ 3.5/5.25 | 0.08/0.07/ 0.06/0.12 | 27/26/25/30 | 420 | no |
| [21] | DMS | 5.5/11.5 | NA | 24/18 | 495 | yes |
| [23] | Slotted Patch Resonator with DGS | 1.85/4.2 | NA | NA | 2200 | yes |
| This Work | DMS | 2.4/3.5/5.2 | 0.3/0.17/0.089 | 40/29/24 | 240 | yes |

reconfigurability, making it adaptable for different applications. It also achieves wider operational bandwidth and wider upper passband solely using one technique "DMS technique". In addition, it can be integrated in the feed line of the antenna, which showcases its efficiency and simplicity.

## 4. CONCLUSION

A low profile BSF with three rejection bands is presented. Three DMSs are etched to produce triple-notched stopbands at Bluetooth (2.4 GHz), Wi-Max (3.5 GHz), and Wi-Fi (5.2 GHz). To enhance the performance of the reflection coefficient $S_{11}$, two dumbbell-shaped DGSs are etched in the ground plane. Three PIN diodes are used to control the band-notched characteristics of the proposed BSF through six states, providing reconfigurability. The lumped element circuit model of the filter has been obtained using ADS, and the results agree well with the CSTMWS. Then, the filter has been fabricated and measured. A 40 dB insertion loss is achieved at 2.4 GHz, 29 dB insertion loss at 3.5 GHz, and 24 dB insertion loss at 5.2 GHz. Moreover, the filter has a rejection ratio of 33.7, 68.38, and 133 at 2.4, 3.5, and 5.2 GHz, respectively. The simulated and measured results exhibit good agreement.

## REFERENCES


1. Rajput, A., M. Chauhan, and B. Mukherjee, "An ultra-wideband bandstop filter with circularly etched stub resonator," *Microwave and Optical Technology Letters*, Vol. 63, 2958–2963, 2021.
2. Islam, H., S. Das, T. Ali, T. Bose, O. Prakash, and P. Kumar, "A frequency reconfigurable MIMO antenna with bandstop filter decoupling network for cognitive communication," *Sensors*, Vol. 22, 6937, 2022.
3. Zuo, X. and L. Qin, "A novel approach to design wideband bandstop filter with wide upper bandpass bandwidth," *AEU-International Journal of Electronics and Communications*, Vol. 138, 153897, 2021.
4. Taibi, A., M. Trabelsi, and A. A. Saadi, "Efficient design approach of triple notched UWB filter," *AEU-International Journal of Electronics and Communications*, Vol. 131, 153619, 2021.
5. Haddi, S. B., A. Zugari, A. Zakriti, and S. Achraou, "Design of a band-stop planar filter for telecommunications applications," *Procedia Manufacturing*, Vol. 46, 788–792, 2020.
6. Ai, J., Y. H. Zhang, K. Da Xu, M. K. Shen, and W. T. Joines, "Miniaturized frequency controllable band-stop filter using coupled-line stub-loaded shorted SIR for tri-band application," *IEEE Microwave and Wireless Components Letters*, Vol. 27, 627–629, 2017.
7. Radonić, V., S. Birgermajer, N. Cselyuszka, and V. Crnojević-Bengin, "Compact dual-band bandstop filter based on coupled open-ended Hilbert resonators," *Journal of Electromagnetic Waves and Applications*, Vol. 33, 1318–1328, 2019.
8. Homayoon, F. and A. A. Heidari, "A band-stop filter based on spoof surface plasmon polaritons using complementary split-ring resonators," *International Journal of RF and Microwave Computer-Aided Engineering*, Vol. 32, e23186, 2022.
9. Cai, Y., K. D. Xu, Z. Ma, and Y. Liu, "Compact bandstop filters using coupled lines and open/short stubs with multiple transmission poles," *IET Microwaves, Antennas & Propagation*, Vol. 13, 1368–1372, 2019.
10. Smari, M., S. Dakhli, E. Fourn, and F. Choubani, "Reconfigurable bandstop filter with switchable CLLs for bandwidth Ccontrol," *Progress In Electromagnetics Research Letters*, Vol. 110, 11–19, 2023.
11. Li, P., Y. Shi, Y. Deng, P. Fay, and L. Liu, "Tunable and reconfigurable bandstop filters enabled by optically controlled switching elements," *Electronics Letters*, Vol. 58, 985–987, 2022.
12. Asci, C., A. Sadeqi, W. Wang, H. Rezaei Nejad, and S. Sonkusale, "Design and implementation of magnetically-tunable quad-band filter utilizing split-ring resonators at microwave frequencies," *Scientific Reports*, Vol. 10, 1050, 2020.
13. Garg, M., R. Chahar, S. Yadav, S. Garg, and D. Noor, "A novel polarization independent triple bandstop frequency selective surface for the mobile and wireless communication," *2017 International Conference on Computing, Communication and Automation (ICCCA)*, 1518–1521, 2017.
14. Zheng, X. and T. Jiang, "Triple notches bandstop microstrip filter based on archimedean spiral electromagnetic bandgap structure," *Electronics*, Vol. 8, 964, 2019.
15. Koirala, G. R. and N.-Y. Kim, "Multiband bandstop filter using an I-stub-loaded meandered defected microstrip structure," *Radioengineering*, Vol. 25, 61–66, 2016.
16. Min, X. and H. Zhang, "Compact triple-band bandstop filter using folded, symmetric stepped-impedance resonators," *AEU-International Journal of Electronics and Communications*, Vol. 77, 105–111, 2017.
17. Elashry, G. M., H. A. Mohamed, A. A. Abd-El-Hadi, and E. A. Abdallah, "Cloverleaf filtenna with reconfigurable quintuple rejection bands using defected microstrip structure," *AEU-International Journal of Electronics and Communications*, Vol. 168, 154708, 2023.
18. Belmajdoub, A., M. Jorio, S. Bennani, A. Lakhssassi, and M. Amzi, "Design of compact microstrip bandpass filter using square DMS slots for Wi-Fi and bluetooth applications," *TELKOMNIKA (Telecommunication Computing Electronics and Control)*, Vol. 19, 724–729, 2021.

19. Hammed, R. T. and B. H. Hameed, "Compact multiple bandstop filter using integrated circuit of defected microstrip structure (DMS) and dual-mode resonator," *AEU-International Journal of Electronics and Communications*, Vol. 107, 209–214, 2019.
20. Rebeiz, G. M., K. Entesari, I. C. Reines, S.-J. Park, M. A. El-Tanani, A. Grichener, et al., "Tuning in to RF MEMS," *IEEE Microwave Magazine*, Vol. 10, 55–72, 2009.
21. Li, Y., W. Li, and Q. Ye, "A reconfigurable triple-notch-band antenna integrated with defected microstrip structure band-stop filter for ultra-wideband cognitive radio applications," *International Journal of Antennas and Propagation*, Vol. 2013, Article ID 472645, 2013.
22. Kingsly, S., D. Thangarasu, M. Kanagasabai, M. G. N. Alsath, R. R. Thipparaju, S. K. Palaniswamy, et al., "Multiband reconfigurable filtering monopole antenna for cognitive radio applications," *IEEE Antennas and Wireless Propagation Letters*, Vol. 17, 1416–1420, 2018.
23. Harikrishnan, A., S. Mridula, and P. Mohanan, "Reconfigurable band stop filter using slotted elliptical patch resonator with defected ground," *2021 6th International Conference for Convergence in Technology (I2CT)*, 1–5, 2021.
24. Costantine, J., Y. Tawk, S. E. Barbin, and C. G. Christodoulou, "Reconfigurable antennas: Design and applications," *Proceedings of the IEEE*, Vol. 103, 424–437, 2015.
25. Gomez-Garcia, R., J.-M. Munoz-Ferreras, W. Feng, and D. Psychogiou, "Input-reflectionless negative-group-delay bandstop-filter networks based on lossy complementary duplexers," *2019 IEEE MTT-S International Microwave Symposium (IMS)*, 1031–1034, 2019.